

# Numerical Investigation of Flow Profile and Performance Test of Cross-Flow Turbine

Nang Saing Nuet<sup>a\*</sup>, Myat Myat Soe<sup>b</sup>, Aung Myat Thu<sup>c</sup>

<sup>a,b,c</sup>Mandalay Technological University, Mandalay and 100/107, Myanmar

<sup>a</sup>Email: nangsaingnuet@gmail.com

<sup>b</sup>Email: myatmyatsoe.mtu@gmail.com

<sup>c</sup>Email: laymyathnar@gmail.com

## Abstract

The paper refers to the numerical analysis of the two stages of inlet and outlet blades of cross-flow turbine. A Computational Fluid Dynamics (CFD) steady state flow simulation has been performed using ANSYS CFX 17. Numerical method has also been used to calculate and predict the efficiency of the turbine. Velocity distribution and within the flow domain has been also characterized. The simulation includes flow domain and blades. The turbine has a specific speed of 44 (metric units), an outside runner diameter of 150 mm. Simulations has been carried out using k- $\epsilon$  turbulence model. The objectives of this study were to analyze the velocity of the Cross-flow within the runner and to characterize its performance for different runner speeds. The CFD simulations results were compared with experimental data and were consistent with turbine efficiency.

**Keywords:** Cross-flow turbine; Numerical analysis; Velocity; Turbine speed; Efficiency.

## 1. Introduction

Recently, small hydro become attractive because of its clean energy sources, renewable and has a good future development. However, the turbine type must be fit to the area conditions of the built turbine. The study or research against the effective and the relatively high production costs with a complex structure are the biggest obstacles to develop small hydro. Small hydroelectric power plants are a solution to the power needs of small communities.

---

\* Corresponding author.

The cross-flow turbine may gain acceptance, and as they can be used in these power plants due to their simple construction, low cost of initial investment and modest efficiency. In order to make them more competitive, it is imperative that their efficiency be improved. This can only be achieved by means of studying the turbine operation and determining the parameters and phenomena that affect their performance. Nowadays, numerical tools are regarded as an industry standard for this process. The improvements in CFD tools have allowed the modeling and obtaining of numerical accuracy of flow fields in turbo machines than previously attained. Turbo machinery designers regularly use numerical methods for predicting performance of hydraulic reaction pumps and turbines. However, numerical methods for predicting the action turbine performance with free surface flow conditions have slowly emerged due to the complex nature of this physic phenomenon.

## **2. Previous Work**

Several studies, both experimental and numerical methods had been done to determine the optimal configuration of the cross-flow turbine. Most of these studies included details concerning the influence of nozzle shape, diameter ratio of the runner, admission arc of the nozzle and the number of blades on the turbine efficiency.

M. Sinagraa, V. Sammartanoa, C. Aricòda [7], they conducted a research on title “Cross-Flow Turbine Design for Variable Operating Condition” in 2013. This paper had outlined a simple but rigorous procedure for the design of a cross-flow turbine with discharge regulator. The researchers had observed reduction of turbine efficiency along with the inlet surface reduction and CFD simulations were also observed.

Vincenzo Sammartano, Costanza Aricò, Armando Carravetta, Oreste Fecarotta and Tullio Tucciarelli [6] they conducted a theoretical framework for a sequential design of the turbine parameters, taking full advantage of recently expended computational capabilities. In this paper a novel two-step procedure was described. In the first step, the initial and final blade angles, the outer impeller diameter and the shape of the nozzle are selected using a simple hydrodynamic analysis, based on a very strong simplification of reality. In the second step, the inner diameter, as well as the number of blades and their shape, are selected by testing single options using computational fluid dynamics (CFD) simulations.

The purpose of the present study is to perform a CFD steady state flow simulation of a hydraulic cross-flow turbine type Banki (including runner blade, and fluid domain) in order to analyze and understand the flow profile of the water flow within the runner. The study is focused on achieving a better use of small hydraulic resources with future cross-flow turbine designs.

## **3. Description of Cross-Flow Turbine**

### ***3.1. Background Theory of Cross-Flow Turbine***

The Banki turbine also known as Cross-flow turbine, named after its inventor, Donat Banki, is a radial-flow wheel and is a variant of a famous undershot waterwheel designed and built by Jean Victor Poncelet. The Poncelet wheel, a vertical one, had an angled sluice generating a broad jet of fluid that intersected the blades of the wheel in a tangential manner. It may be regarded as an early pressureless turbine. Poncelet’s results of his theoretical and experimental studies were published in 1825, for which he was awarded the Mechanical Prize of

the French Royal Academy of Sciences. Thereafter many Poncelet turbines were built and operated successfully. The Banki turbine has a characteristic speed range between that of a Pelton wheel and a Francis turbine. Mockmore and Merryfield (1949) have made a thorough investigation of its characteristics. The turbine, schematically shown in Figure 1, consists of a wheel, like Poncelet's, with curved blades around the periphery. One of the differences is the mechanism of flow control.

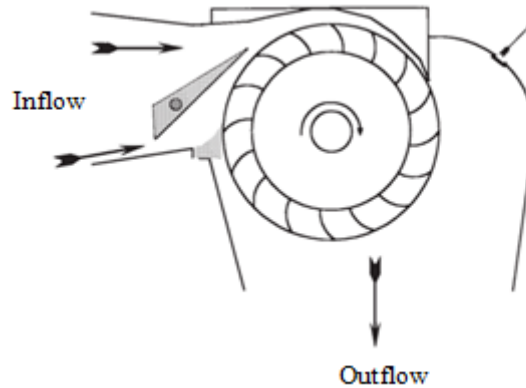


**Figure 1:** Schematic Diagram of Cross-Flow Turbine [9]

### **3.2. Cross-Flow Turbine Physical Description**

The components of this machine are runner, nozzle, blades, shaft, bearing, casing, draft tube, guide vane and air valve which are described in Figure 1.

The heart of the any turbine is runner. The runner has the shape of an empty wheel, consisting of two circular plates linked by a series of blades, shaped so that the jet is directed towards the center of the wheel and then again crossing other blades before exiting. The jet then passes through the runner and this is the origin of the name “cross-flow”. The runner is connected to the generator for the electricity production. The function of the runner is the conversion of water energy into mechanical energy. In the case of wider runner, the blades have multiple interposed by the supporting board.

In the Cross-flow turbine, nozzle is rectangular shape that its width matches width of runner. Its main function is to convert the total available head into kinetic energy and to convey the water to the runner blades. It is mounted at the end of penstock and their exit is placed very close to the outer periphery of the turbine runner.

### **3.3. Flow through Cross-Flow Turbine**

There are two major flow patterns through a cross-flow turbine, cross flow and entrained flow shown in Figure 2. When water follows the cross flow pattern from point 2 to 3, it hits the turbine blades at two stages before it exit the turbine. The angle and curvature of the blades are designed so the water will transfer a significant amount of torque at stage two at point 3 before exiting the turbine.

A part of the flow is trapped by the blades and swung around to the bottom of the turbine. This is what is called entrained flow. This flow pattern will only contribute with one stage of torque transfer. Rotational speed of the rotor and nozzle opening affect the cross flow through the runner. Inappropriate configuration of the turbine can make the water hit the axle or most of the flow gets entrained.

Leakage flow is a loss due to water flowing through gaps between the rotor and turbine casing. There are two leakage flows, one between the end of the top cover. The other leakage flow is between the side casing and the rotor. Lower tolerances in the manufacturing will give less leakage flow.

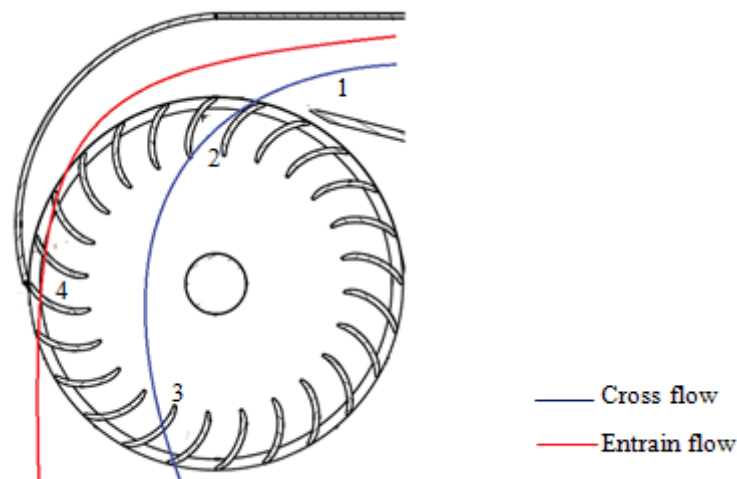


**Figure 2:** Flow through Cross-Flow Turbine [10]

#### 4. Model Cross-Flow Turbine Description

The dimensions of the Cross-flow turbine used in this study are those of the actual Cross-flow turbine that tested at Renewable Laboratory at the Mandalay Technological University, Myanmar. The performance test established the best efficiency point.



**Figure 3:** Cross-Flow Turbine

The performance of the turbine with varied head, flow and runner speed from the best efficiency point. The

experimental results are used to validate the numerical results on performance assessment. The best operating point of 72% was identified at 4.79 m head, 162 rpm and a manual valve opening of 7 cycles. The normalized design parameters are given in Table 1 and the experimental set-up of Cross-flow turbine is shown in Figure 4.

**Table 1:** Design Parameter of Cross-flow Turbine

N0.	Description	Symbol	Value	Unit
1.	Outer diameter of runner	$D_1$	150	mm
2.	Inner diameter of runner	$D_2$	100	mm
3.	Width of runner	$B_0$	76	mm
4.	Angle of attack	$\alpha_1$	16	degree
5.	Radius of blade curvature	$R_{bc}$	24.46	mm
6.	Radius of pitch circle	$R_0$	55.35	mm
7.	Radial rim width	a	25	mm
8.	Central angle of each blade	$\delta$	73	degree
9.	Spacing of blade in wheel	t	22.5	mm
10.	Inlet blade angle	$\beta_1$	30	degree
11.	Number of blade	z	20	-
12.	Width of nozzle	b	57	mm



**Figure 4:** Experimental Set-up of Cross-flow Turbine

## 5. Experimental Test Case

The simplified Cross-flow turbine with a specific speed of 44 (metric units) is used as the test object. This facility was designed to characterize the performance of the turbine. Through the tests were obtained the global performance parameters of the turbine for different runner speeds, at each flow rate and head tested. With the

processing of all this data, the hill diagram of the turbine was constructed.

**5.1. Calculation of Effective Head and Efficiency**

The effective head at inlet to the turbine can be measured through use of Bernoulli equation; the result given in the equation (1), which expresses that the energy acquired from the fluid that flows through the runner is a function of the angular moment variation.

$$H_e = \frac{P}{\rho g} + \frac{V^2}{2g} + Z \tag{1}$$

Where  $V_1$  is the velocity of water at inlet to the turbine (m/s),  $P_1$  is the gauge in pressure (N/m<sup>2</sup>) at point inlet and  $Z$  is the height difference (m) between the pressure transducer and the centre of the Cross-flow turbine runner.

The global efficiency of the turbine is given by (2). Furthermore, for this study it is important to mention the hydraulic efficiency, which considers the losses due to hydraulic effects. The turbine efficiency can be expressed as

$$\eta = \frac{P_{Shaft}}{P_{Hydraulic}} = \frac{T_s \omega}{\rho g Q H_e} \tag{2}$$

where  $P_{Shaft}$  shaft power (W),  $P_{Hydraulic}$  is the hydraulic power (W),  $T_s$  is shaft torque (Nm);  $\omega$  is runner angular velocity (rad/s),  $\rho$  is the density of water (kg/m<sup>3</sup>),  $g$  is the acceleration due to gravity (m/s<sup>2</sup>),  $Q$  is the water flow rate (m<sup>3</sup>/s) and  $H_e$  effective head (m). The experimental Data and Result are shown in Table 2.

**Table 2:** Experimental Data and Result

Gate valve adjustment, (cycle)	Flow rate, (m <sup>3</sup> /s ×10 <sup>-3</sup> )	Turbine inlet pressure, (kPa)	Runner speed, (rpm)	Effective Head, (m)	Output Power, (W)
2-cycle	3.65	17.23	93	2.1	38.4
3-cycle	4.29	24.13	110	2.87	57.8
4-cycle	4.71	31.03	128	3.62	106
5-cycle	5	33.09	145	3.86	126
6-cycle	5.26	34.47	157	4.04	153
7-cycle	5.48	37.92	162	4.42	169
8-cycle	5.65	41.37	166	4.79	175

## 6. Numerical Approach

In general, a numerical analysis procedure involves the following steps: (i) development of governing equations for the flow physics; (ii) discretising the equations in both time and space, (iii) discretising the flow domain (meshing), (iv) solving the discretised equations using a computerised solver, and (v) post-processing of the results using a computerised program. It is necessary to justify the numerical results by comparing them with experimental or theoretical results. As stated already, numerical analysis is currently the standard way of designing turbines in the industry. Numerical analysis for predicting the performance of impulse turbine runners poses a special challenge because of complexity of the flow physics. In impulse turbines like Pelton turbine, the jet flow in the runner is intermittent, and there is a movable free surface boundary between the jet and surrounding air. This means that the actual flow is unsteady and two phase with a movable free surface. Two approaches are being used to numerically analyse such a flow. These approaches are particle tracking method and a classical CFD method [10Pat].

### 6.1. Design Modeler and Meshing

The numerical analysis for this study was performed in ANSYS Workbench 17 where ANSYS CFX Project with its subprograms, namely: Geometry, Mesh, ANSYS CFX-Pre, ANSYS CFX solver and ANSYS Post-processing, was used. As stated already, numerical analysis require coming up with a flow domain which has to be meshed. The flow domain shows in Figure 5 was designed in 'Geometry' sub-program using the ANSYS Design Modeler. The flow domain consists of the blades, fluid domain. The blade was designed in AutoCAD 2014. In the ANSYS Design Modeler, the blade was imported and positioned at the required central position. This numerical analysis involves the blades, which have a rotating frame of reference while the inlet and outlet of fluid domain have non-rotating frame of reference (stationary frame of reference).

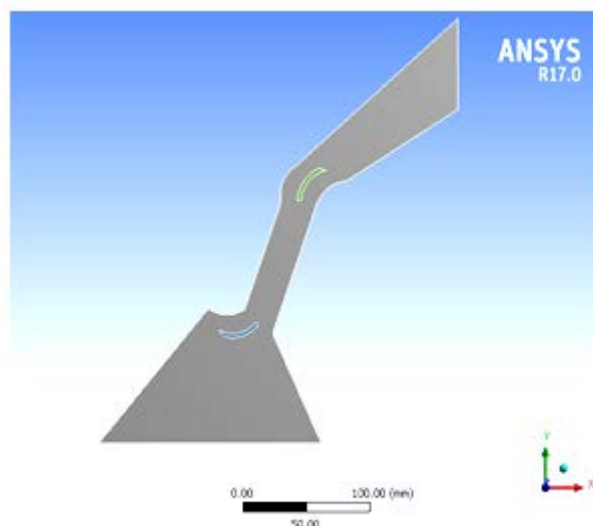


**Figure 5:** Flow Zone Diagram of Inlet, Outlet and Blade

The flow domain was meshed using the ANSYS Mesh sub-program of the ANSYS CFX Project. The mesh properties are given in Table 3. The number of mesh elements for the final numerical analysis reported in this study was 23080, is a good number of mesh for the simulation. Large number of mesh elements would cause a delay in the convergence of the solution. In the mesh, the relevance centre fine was employed to ensure relatively high accuracy of calculated results for the blade model. Table 4 shows mesh statistics for the three computational zones.

**Table 3:** Mesh Properties used in the Ansys CFX

Mesh property	Value/Action
Use advanced size function	On Proximity Curvature
Relevance Centre	Fine
Initial size seed	Active Assembly
Smoothing	Fine
Transition	Fast

**Table 4:** Mesh Number of Element

Domain	Nodes	Elements
Blade1	10850	8280
Blade2	10812	8308
Fluid Domain	8034	6492

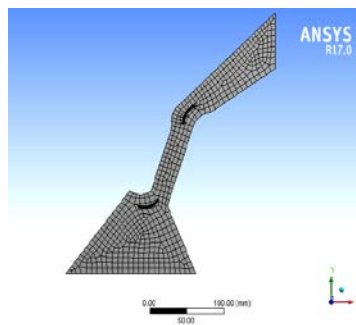


**Figure 6:** Meshing of Flow Physics

## 6.2. Boundary Condition and Interface

Modeling of the flow physics included creating interfaces for flow zones (or domains), assigning boundary conditions, assigning initial conditions, applying governing equations with appropriate turbulence models and choosing the flow materials (water and air) and their phase properties. The solution control and declaration of variables were also done in the ANSYS CFX-Pre. The domains were interfaced using the rotational periodically



model in the ANSYS CFX-Pre. The boundary conditions were prescribed at inlet, outlet, wall and the interface locations of the blade, as shown in the above Table 5. Mass flow rate has been defined at the inlet and pressure at the outlet. A reference frame has been created with experimental data rpm and has been assigned to the rotating blades.

**6.3. Turbulence Model**

In the computational process the k-ε (k-epsilon) turbulence model was used. One of the most prominent turbulence models, the k-ε (k-epsilon) model, has been implemented in most general purpose CFD codes and is considered the industry standard model. It has proven to be stable and numerically robust and has a well-established regime of predictive capability. For general purpose simulations, the model offers a good compromise in terms of accuracy and robustness [14].

**Table 5:** Boundary Physics for Blades, Inlet and Outlet

Location	Assigned boundary condition type	Boundary condition details	
Inlet	Inlet	Domain type	Fluid domain
		Frame type	Stationary
		Flow region	Subsonic
		Domain motion type	Stationary
		Mass and momentum option	Mass flow rate
		Heat transfer	Stationary Frame total temp, (288.13K)
Outlet	Outlet	Domain type	Fluid domain
		Frame type	Stationary
		Flow region	Subsonic
		Domain motion type	Stationary
		Mass and momentum option	Average static pressure, Relative pressure 1 atm
Blade	Wall	Frame type	Rotation
		Mass and momentum option	No slip wall
		Wall roughness option	Smooth
Side 1 and Side 2	Wall	Frame type	Rotation
		Mass and momentum option	No slip wall

After set up the boundary conditions in ANSYS CFX-Pre, the solutions were run in CFD Post. The maximum iteration is 500 and the convergence is occurred at about 300 as shown in Figure 7.

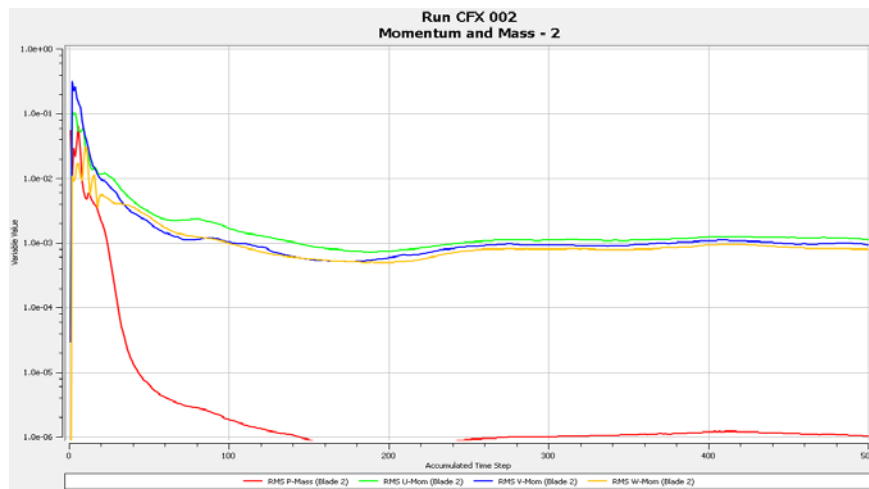


**Figure 7:** Graph of Mass and Momentum during Simulation against Number of Iteration

## 7. Result and Discussion

Velocity contours were obtained using insert contour and location commands of menu bar in ANSYS CFX-Post. Figure 8 shows the velocity contour in the flow field of the blade model. The velocity contour, it is seen that the inlet velocity is higher than the outlet velocity. In the following set of Figures, the velocity contours at mid span for different runner speeds (93, 110, 128, 145, 157, 162 and 166 rpm) are shown in Figure 9 and Figure 10. It is seen that the jet coming out of higher velocity rate that velocity contours before striking the blade at the first stage. The velocity contour across the flow area is obtained along the fluid domain. The velocity contours at the inlet of the blade having 7.1 m/s, 8.4 m/s, 9.5 m/s, 10.5 m/s, 11.2 m/s, 11.6 m/s and 11.9 m/s and blade outlet velocities 3.559 m/s, 4.21 m/s, 4.77 m/s, 5.25 m/s, 5.6 m/s, 5.8 m/s and 6 m/s with runner speeds (93, 110, 128, 145, 157, 162 and 166 rpm) respectively.

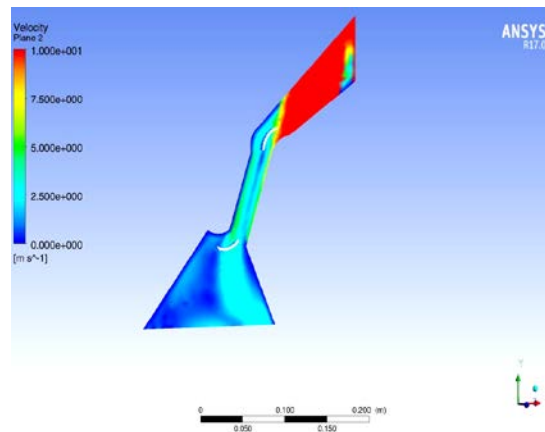
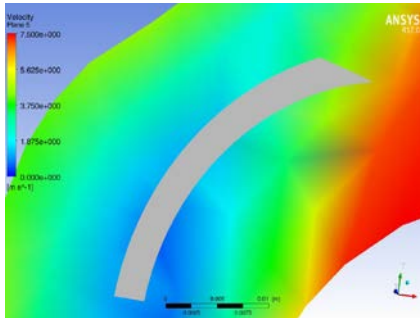
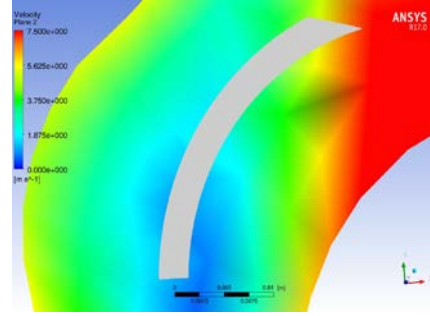


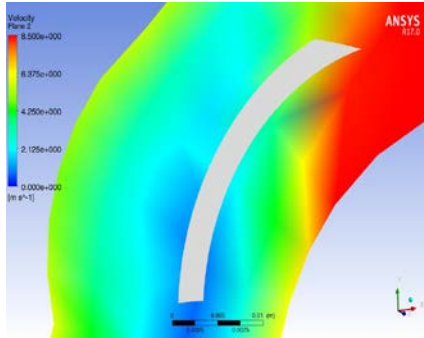
**Figure 8:** Velocity Contour in Fluid Domain



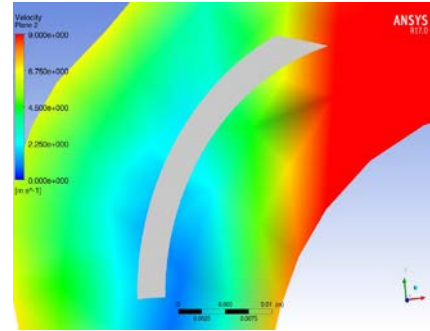
(a) 93 rpm



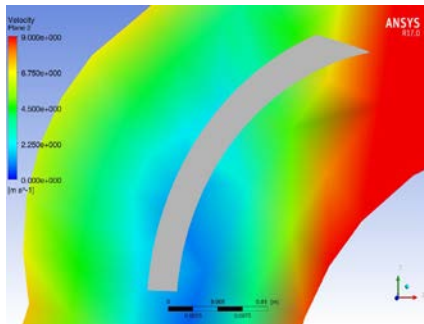
(b) 110 rpm



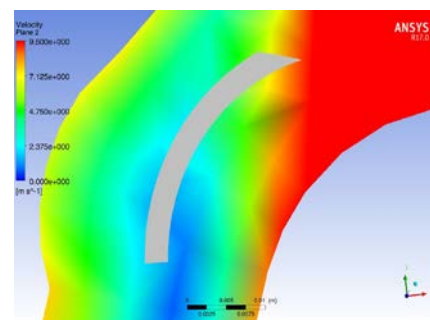
(c) 123 rpm



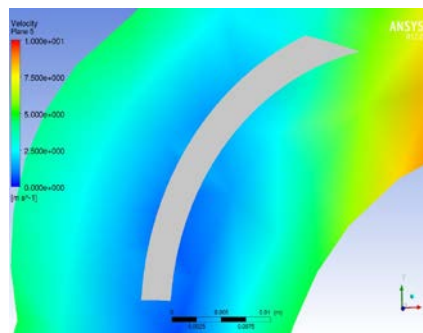
(d) 145 rpm



(e) 157 rpm

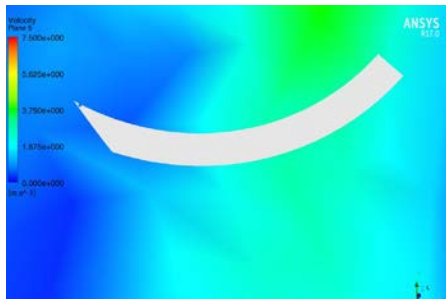


(f) 162 rpm

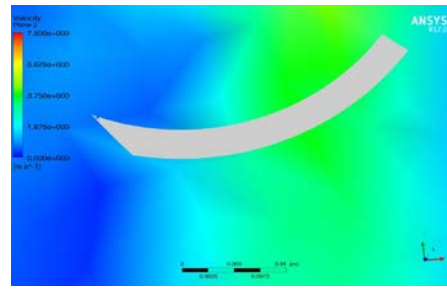


(g) 166 rpm

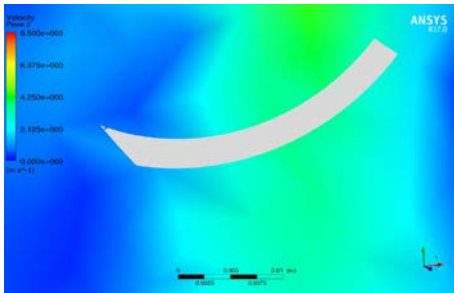
**Figure 9:** Velocity Contour for Various Speeds in Blade Inlet



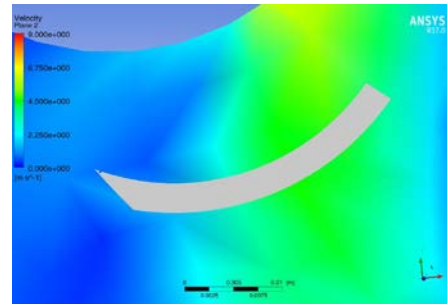
(a) 93 rpm



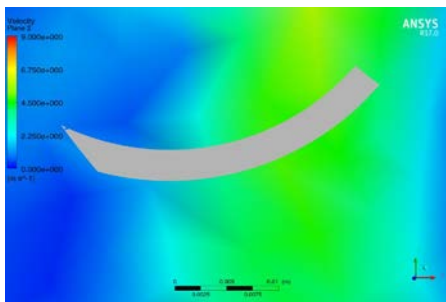
(b) 110 rpm



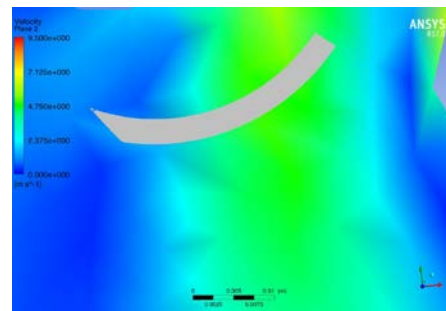
(c) 128 rpm



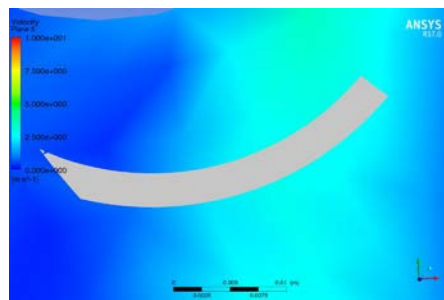
(d) 145 rpm



(e) 157 rpm



(f) 162 rpm



(g) 166 rpm

**Figure 10:** Velocity Contour for Various Speeds in Blade Outlet

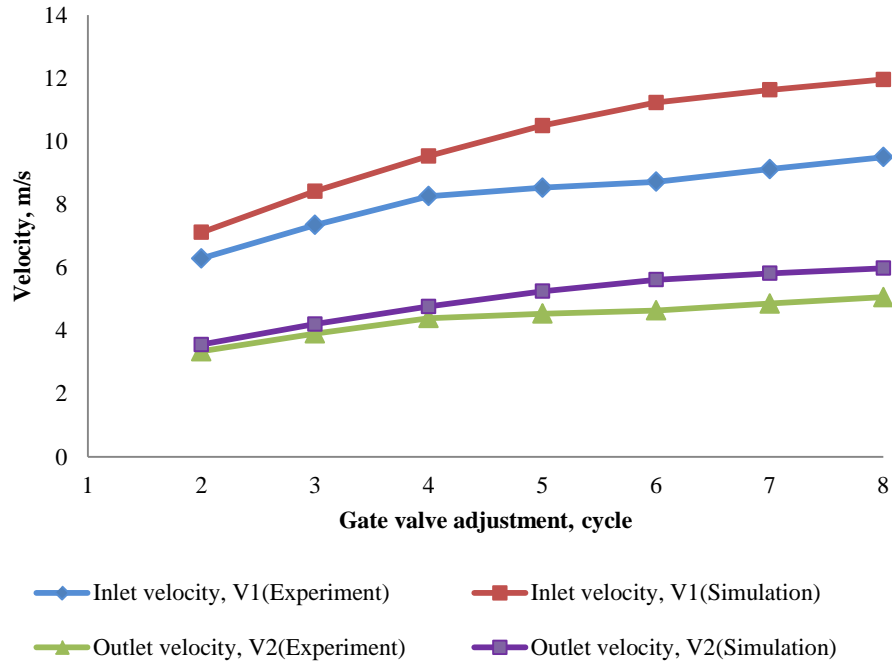


**Figure 11:** Variation of Turbine Efficiency with Gate Valve Adjustment

It can be seen from Figure 10 that the graph for experiment result of inlet velocity and outlet velocity, numerically determined inlet velocity and inlet velocity show similar trends. The numerically determined inlet velocity and outlet velocity tends to give higher values especially for gate valve five cycles opened condition, thus indicating that numerical analysis over predicts the performance.

Numerical analyses are associated with numerical errors and it is difficult to describe mathematically some flow processes. Numerical errors arise from the numerical procedure, mesh, data processing and geometric complexity of the turbine. Further, assumptions on the boundary conditions and turbulence model are major sources of numerical errors and may generate unrealistic simulation results.

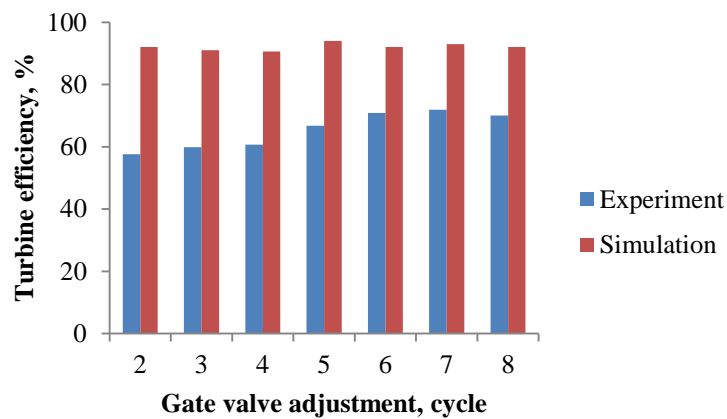


**Figure 12:** Variation of Turbine Efficiency with Gate Valve Adjustment

## 8. Conclusion

In this study the experiment of cross-flow turbine has been carried out. In this experiment the maximum effective head 4.79 m and maximum flow rate  $5.65 \times 10^{-3} \text{ m}^3/\text{s}$  were occurred at gate valve fully open. The variable speeds of the turbine are between 93 and 166 rpm depending on the flow rate. Moreover, the numerical analysis (velocity distribution) has been presented. The flow velocity at the inlet of the nozzle is constant and it is going to increase inside the nozzle nearer to the first stage runner blades and then going to decrease at the second stage out let of the turbine. According to the theory result, the maximum turbine efficiency is 71.6%. According to the numerical result the maximum turbine efficiency is 94%.

## Acknowledgement

The author is deeply gratitude to Dr. Myint Thein, Rector, Mandalay Technological University, for his guidance and advice. The author gratefully acknowledge to Dr. Tin San, Associate Professor and Head of Mechanical Engineering Department, Mandalay Technological University. The author would like to express grateful thanks to her supervisor Dr. Myat Myat Soe, Associate Professor, Department of Mechanical Engineering, and to all her teachers from Mandalay Technological University. The author's special thanks are sent to her parents for their guidance from childhood till now.

## References

- [1] N. Acharya, C. G. Kim and B. Thapa, Y. H. Lee, "Numerical Analysis and Performance Enhancement of a Cross-flow Turbine," ELSEVIER, January 2015.
- [2] N. S. Nuet, M. M. Soe and M. M. Htay "Design Optimization and Flow Analysis on the Runner Blade of Cross-Flow Turbine", ICSE, December, 2015.
- [3] C. S. Kaunda, C. Z. Kimambo and T. K. Nielsen, "A Numerical Investigation of Flow Profile and Performance of a Low Cost Cross-flow Turbine," IJEE, vol. 5, pp. 275-296, 2014.
- [4] C. S. Kaunda, C. Z. Kimambo and T. K. Nielsen, "Experimental Study on a Simplified Cross-flow Turbine," IJEE, vol.5, pp. 155-158, 2014.
- [5] M. Girma and E. Dribssa, "Flow Simulation and Performance Prediction of Cross-flow Turbine Using CFD Tool," IJER, vol. 2, pp. 747-757, Oct. 2014.
- [6] V. Sammartano, C. Arico, A. Carravetta and O. fecarotta, "Banki-Michell Optimal Design by Computational Fluid Dynamics Testing and Hydrodynamic Analysis," ISSN, vol. 6, pp. 2362-2385, Jun. 2013.
- [7] M. Sinagraa, V. Sammartanoa, C. Aricòda, "Cross-Flow Turbine Design for Variable Operating Condition", ELEVIER, pp. 1539-1548, 2013.
- [8] Bilal Abdullah Nasir, "Design of High Efficiency Cross-flow Turbine for Hydropower Plant," IJEAT, vol. 2, pp. 308-310, Feb. 2013.
- [9] G.F.Round, "Incompressible Flow Turbomachine" ELSEIVER, 2014.
- [10] M. A. Just and G. S. Saabye, "Assesment of Structural Integrity and Potential Improvements of Micro Hydropower Turbine", The Norwegian University of Science and Technology, June, 2013.

- [11] J.D. Andrade, C.Curiel, F. Kenery, O.A.A. Vasquez and M. Asuaje, "Numerical Investigation of the Internal Flow in a Banki Turbine," IJRM, vol 2011, P-12.
- [12] M. Nechleba and Dr. Techn, "Hydraulic Turbines", 1957.
- [13] C.A. Mockmore, "The Banki Water Turbine", Bulletin Series No. 25, 1949.
- [14] <http://www.ansys.com>, ANSYS CFX Solver Modeling Guide, 2015.
- [15] <http://www.ansys.com>. ANSYS CFX Pre User's Guide, 2015.
- [16] <http://www.ansys.com>. ANSYS CFX Solver Theory Guide, 2015.